MATERIAL TESTS FOR TEXTURED SILICONE RUBBER SAMPLES

P.Charalampidis*, R.T.Waters, A.Haddad, H.Griffiths, N.Harid and P.Sarkar
High Voltage Energy Systems Group, School of Engineering, Cardiff University,
The Parade, Cardiff, CF24 3AA, UK
*Email: <charalampidisp@cardiff.ac.uk>

Abstract: Inclined-plane tests of silicone-rubber samples prepared with textured patterns of hemispherical protuberances are described. These are compared with the results obtained for conventional non-textured plane-surface samples of the same material. A remarkable improvement is achieved by such texturing: a material which normally fails the test is enabled to satisfy the standard test criteria, and the tracking and erosion of the samples caused by the tests are significantly reduced. These texturing techniques are currently being extended to prototype composite insulators.

1 INTRODUCTION

For the pollution and moisture conditions that prevail in coastal / industrial regions, a significant leakage current may occur before sufficient transfer of hydrophobicity from the surface of a silicone-rubber insulator to an overlaying pollution layer can be established [1]. The surface leakage current density J in the pollution layer is highest at the shank region between sheds, which also results in an enhanced electric field strength E at the same location; these conditions lead to a cascading effect of increased surface heating (the surface power density is $P = EJ$), followed by dry band formation and consequent discharges over the surface.

Silicone rubber to be moulded for insulator manufacture is required to possess discharge-resistant qualities. To optimize the formulation, it is common practice to subject rectangular samples (120 mm × 50 mm × 6 mm) of material to tests according to IEC 60587 [2], which evaluates the resistance to tracking and erosion properties of the silicone rubber formulation. Part A of this paper reports test outcomes not only with standard silicone-rubber samples but also with samples that have been prepared with a modified surface. This modification is possible because, unlike ceramic or glass materials, the surface of a polymeric insulator can be finely textured [3] in ways that are compatible with moulding. The objective of this texturing is to achieve an increased leakage current path length and surface area, thereby reducing both the leakage current density J and the electric stress E.

The optimization of the texture for prototype insulator development is reported in this paper. Three different surface geometries, each of which employs a different pattern of hemispherical protuberances, have been chosen for study: <u>Texture α</u> is a contiguous hexagonal pattern; <u>Texture β</u> comprises hexagonal intersections of overlapping protuberances; and <u>Texture γ</u> is an intersecting square arrangement. A detailed analytical study of the texture design has been reported elsewhere [4]. In addition to the chosen surface textures, a range of diameters of the hemispherical protuberances were used (2 mm, 4 mm, 6 mm, 8 mm and 10 mm). This paper compares the inclined-plane test results obtained with samples of the above-mentioned textures and with non-textured plane samples.

Additional observations were performed in order to interpret the test results, in which the discharge activity was monitored using a FLIR A325 infrared camera. This has proved to be a particularly useful addition to the standard test, because the surface heating of the sample, resulting from both the current in the polluted layer and that associated with electrical discharges, can be recorded. For some tests, a high-speed visible-spectrum camera was also used. Texturing of the silicone rubber is shown to inhibit arcing by promoting the formation of stable dry bands. Discharges across these bands reduce, rather than increase, the leakage current of the sample.

Finally, comprehensive high-resolution data logging of the leakage current characteristics provides new information on the discharge parameters, which allows their physical properties to be quantified and physical models to be tested.

2 TEST PROCEDURE

IEC 60587 specifies that the rectangular sample must be inclined at angle of 45° to the vertical with the test side facing downward. A power-frequency test voltage of 3.5 kVrms is applied across electrodes which are 50 mm apart. A specified contaminant (a solution of distilled water with 0.1 % concentration of ammonium chloride and 0.02 % of non-ionic wetting agent Trixton-100) flows from the high-voltage upper electrode through a notch, and traverses the test surface at a volume flow rate of

0.3 ml/min for the duration of the test. The leakage current during these tests was logged with a NI (National Instrument) data acquisition board (see 6.1). The specified criteria required to pass the IEC 60587 test includes the limit that the current should not exceed 60 mA for any period of 2s during a 6 hour test.

3 SAMPLE PREPARATION

The samples were prepared using liquid silicone-rubber Dow Corning HV 1540/10P and the moulding process was accomplished using a vacuum casting machine. The properties of liquid silicone rubber HV 1540/10P are given in [4]. For producing these samples, an aluminium cast tooling plate was used to fabricate the moulds as negatives of the samples. Either contiguous or intersecting blind holes were drilled with hemispherical cutting tools using a CNC machine to give the required protuberance pattern over the surface of the rectangular sample. Examples of a mould and a silicone rubber test sample are shown in Figure 1.

4 RESULTS OF INCLINED-PLANE TESTS

Table 1 summarises the IEC 60587 inclined-plane test data for both non-textured and textured rectangular samples. These results provide a strong corroboration of the anticipated improvement in performance associated with the surface texturing of the silicone rubber.

The 100% success rate of the three patterns tested, for all five sizes of protuberances, contrasts with the consistent failure of the same material with a plane surface.

Further investigations, to augment these standard tests, were undertaken to interpret this remarkable outcome and ancillary monitoring and measurements have proved to be extremely informative in explanation of the results of Table 1. The infrared camera was useful to interpret normal photography of surface discharges, whose luminosity was relatively faint in the visible spectrum, and these observations are described in Section 5.

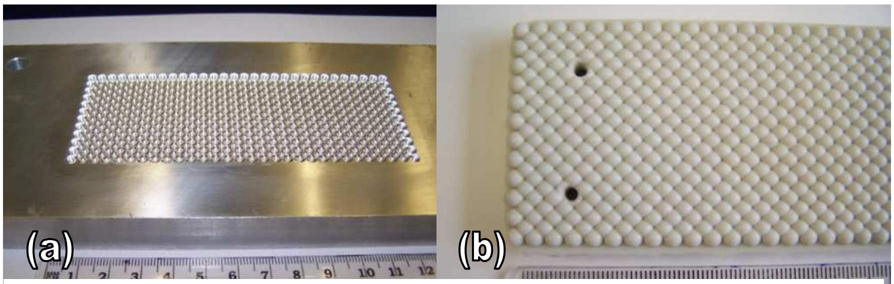

Figure 1: Preparation of test sample with a textured surface. a) Cast-aluminium mould for rectangular test sample and (b) silicone-rubber test sample 4 mm square pattern (Texture γ).

Table 1: Inclined-plane test data.

Protuberance diameter (Texture type)	*Number Tested*	*Pass*	*Fail*	*Fail time (minutes)*		*Maximum current (mA rms)*	*Track length (mm)*		*Erosion depth (mm)*		*Weight loss (g)*	
				Min	*Max*		*Min*	*Max*	*Min*	*Max*	*Min*	*Max*
Plane non-textured sample	**6**	**0**	**6**	40	180	> 60.0	42.0	47.0	5.0	6.0	2.5	3.0
2 mm (γ)	**4**	**4**	**0**	-	-	38 – 44	20.0	24.0	4.0	5.0	1.5	2.5
4 mm (α)	**4**	**4**	**0**	-	-	34 – 37	20.0	24.0	3.0	5.0	1.0	1.5
4 mm (β)	**4**	**4**	**0**	-	-	42 – 47.5	6.0	18.0	1.0	3.0	0.5	1.2
4 mm (γ)	**8**	**8**	**0**	-	-	40 – 43	5.0	15.0	<1.0	3.0	small	0.5
6 mm (γ)	**6**	**6**	**0**	-	-	40 – 44	6.0	20.0	<1.0	5.0	small	1.1
8 mm (γ)	**4**	**4**	**0**	-	-	38 – 42	18.0	23.0	3.0	5.0	1.3	1.5
10 mm (γ)	**4**	**4**	**0**	-	-	45 – 50	15.0	24.0	4.0	5.0	1.4	1.5

5 VISIBLE AND INFRARED RECORDS

5.1 Non-Textured Plane Surface

An example of the rms leakage current for the duration of a test on a plane surface (in this case the duration was 40min followed by failure) together with the discharge activity as monitored by the infrared camera is shown in Figure 2. The flow of the contaminant stream down the sample remained narrow throughout, as indicated by the heated area of the conducting layer in Figure 2(b). The IR camera indicated a maximum contaminant temperature of 70^{o}C.

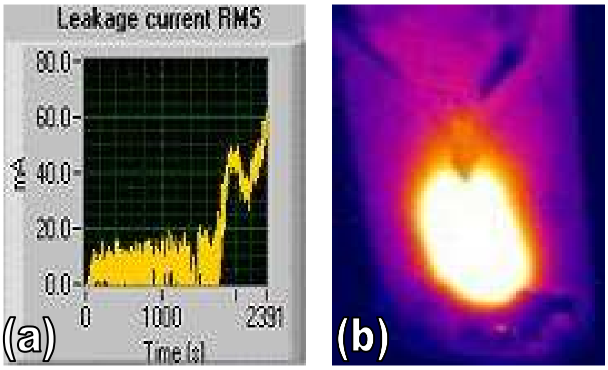

Figure 2: Non-textured sample progression to failure. (a) LabVIEW record of rms leakage current over test duration and (b) infrared image showing anchored arc.

Dry bands were readily formed at or near the ground electrode, and these were often bridged by unstable arc-like discharges causing deep erosion. Test failure invariably followed.

5.2 2mm Square Pattern (Texture γ)

For the textured samples, arcing was significantly reduced. Instead, the formation of dry bands with associated discharge activity was evident both visually and, especially, in the infrared. Because the shape of the standard high-voltage electrode created a severe voltage gradient adjacent to it, a dry band first formed in that area. Three unique characteristics were associated with its formation: first, a line of short, parallel and dynamic streamer-type discharges formed across the width of the dry band, so rendering the dry band visible; secondly, the onset of these discharges was accompanied by a fall, rather than an increase, of current; and thirdly, the dry band and its line of discharges advanced along the sample surface in the direction of the contaminant flow towards the ground electrode. Although this advance was caused by the contaminant flow, the rate of progress was slower than the flow rate, so that some seconds were needed to traverse the sample.

The contaminant flow, beginning as before in a narrow stream, soon spread across the width of the sample in a way not found with a plane surface. The infrared camera detected the ohmic heating of this wider conduction region.

Figure 3 shows infrared images of these dry-band discharges. Extinction of the discharges during the advance was frequently followed by reignition, which suggested temporary bridging of the dry band by the contaminant flow. If the discharge activity reached the ground electrode, it became concentrated to cause some limited erosion of insulating material from that region.

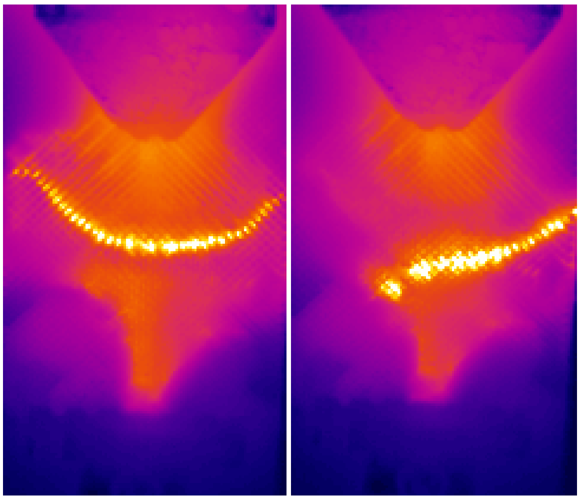

Figure 3: Infrared images of progression of dry-band discharges Texture γ, 2mm).

5.3 4mm Hexagonal Pattern (Texture β)

As before, there were faint discharges spread across the width of the sample moving in parallel along the intersecting edges of the hemispheres towards the ground electrode. The onset of these discharges was again associated with a reduction in the leakage current. For these samples, a fast camera of 1000 fps with an exposure time of 1 ms was available, and although resolution was poor, it was established that 2-3 faint streamers were recorded per frame. Near the ground electrode there were more intense arc-like discharges, but these were distributed across its width resulting in a smaller loss of insulating material than by the anchored arc of the plane sample.

5.4 4mm Square Pattern (Texture γ)

The faint discharge activity again spread across the width of the sample accompanied by a fall of leakage current when the discharges were present. Close inspection showed that the discharge channels across the dry band formed along the intersecting edges of the hemispherical protuberances. In the square pattern all intersections are aligned at 45 degrees to the electric field direction. The discharges, as seen by eye, are shown in Figure 4. These constricted channels rich in UV are typical in appearance of streamer growth. The length of an individual discharge channel can increase when the dry band approached the ground electrode, where the discharges tend to jump the protuberances. Again, the rate of movement of the dry band and its discharges is slower than the rate of flow of the contaminant across the sample. The time taken by a drop of contaminant to flow from the HV electrode notch to the ground electrode was about 5 seconds, whereas the progress of the discharge phenomena could last for up to 17 seconds for this texture.

As before, it was observed that the leakage current was at its peak just before the start of the discharge phenomena. The current distribution was evenly spread across the width of the sample as indicated by the heating observed by the infrared camera. These discharges again usually started from the HV electrode and subsided on reaching near the ground electrode. During the transit, discharges across the dry band were again often briefly interrupted. The IR images of such a progression are shown in Figure 5. This process of dry band motion across the sample was repetitive, but in between there were some time gaps before the launch of a new dry band during which there was no activity (dark periods) and the leakage current was negligible. This was attributed to the persistence of a dry band in the eroded region near the ground electrode. Near the ground electrode, the discharges took the form of mobile arcing evenly spread along the width of the sample which caused negligible loss of material. A second fast camera, operating at 2000 fps and exposure time of 0.5 ms, was employed to monitor the discharge activity. These photographs again showed that only 1-3 dry-band discharges were active per half-cycle of current.

5.5 6, 8 & 10mm Square Pattern (Texture γ)

For 6mm protuberances, faint discharge activities were again observed spread across the width of the sample, with a reduction in leakage current. These bridged the dry band, individual discharges being directed along the intersecting edges of the hemispheres, and the dry band moved towards the ground electrode as in the 4 mm textured square-pattern case.

For 8 and 10mm protuberances, however, very few discharges were observed. Intermittent discharges were quite random unlike the smaller square-pattern textured samples. This indicates either that a stable dry band was not formed in these cases, or that the applied voltage of 3.5kV was too low to bridge such bands by streamer breakdown. Near the ground electrode, there was intense arcing concentrated in few places which caused a greater loss of insulating material.

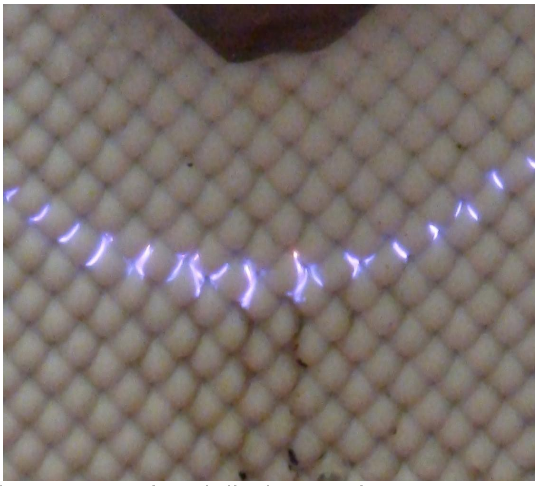

Figure 4: Dry-band discharges (Texture γ, 4mm)

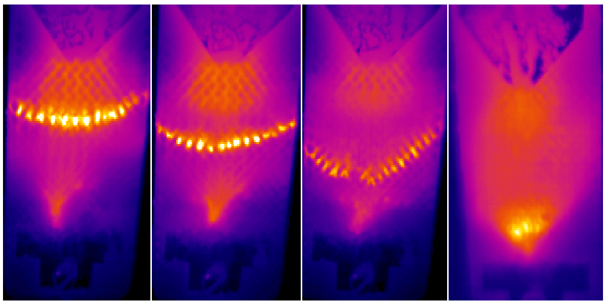

Figure 5: Infrared image of discharge activity progression (Texture γ, 4mm)

6 CURRENT MEASUREMENTS

6.1 Data Acquisition and Multi-Path Currents

For a more detailed insight of the formation of conductive paths, the IEC-60587 standard test was modified by replacing the single ground electrode with five smaller, isolated and adjacent electrodes to explore multi-path current flow on the textured surface [Figure 6].

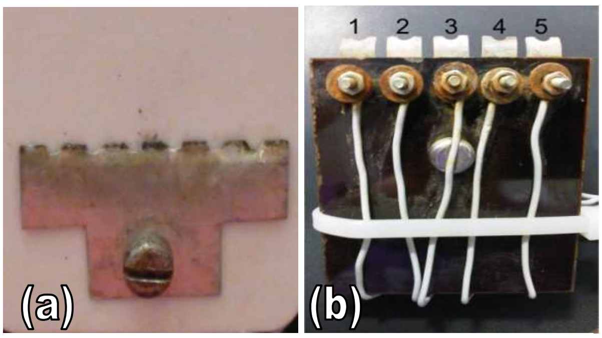

Figure 6: (a) Single ground electrode as specified by IEC-60587 and (b) the modified ground electrode consisting of five smaller isolated electrodes.

In addition, a Data Acquisition (DAQ) system was designed for the tasks of controlling the inclined plane test machine, acquiring the values of the test parameters and logging and interrogating the data. The test voltage and the five leakage-current signals were driven to a National Instruments data acquisition board (NI PCI-6254) that converts the signal to digital information for input to a PC. The physical connection of the input signals with the DAQ board took place through a SCB-68 connector block.

The software was developed with National Instruments LabVIEW version 2009. The program terminates the test when the total leakage current exceeds 60mA for 2s (in accordance to IEC-60587 method A end point criterion) or when 6 hours of testing has elapsed. Five charts indicate the history of rms values of leakage current for each electrode and one chart indicates the total leakage current history. A typical record is shown in Fig.7.

The graphical LabVIEW code was developed by implementing Producer/Consumer and State Machines architectures [5]. Each of the six analog inputs (voltage and five leakage current signals) were sampled at a rate of 104 samples per second resulting in the capture of 200 samples per cycle for the power supply frequency (50Hz). The data were saved into TDMS files [6] with each file containing 6 columns representing the six input channels.

The inclined-plane test posed the challenging demands of the acquisition of large amounts of data over a prolonged test, with the need to facilitate data retrieval with good time resolution. To meet this, the program opens a file to a user specified location and when 60x103 samples of each channel have been logged into the file, the latter closes and a new file is created to store the next segment of incoming data, thus saving 6 seconds of real time test data. The increment is 100µs which is the time elapsed between two acquired samples. For a standard six hours test, $36\mathrm{x}10^{2}$ files are created.

The saved data was post-processed to display a number of properties such as FFT analysis (not shown here) and energy dissipation.

6.2 Current History in Inclined-Plane Tests

Figure 7 shows the leakage current distributions (a) on a plane non-textured sample that failed the test after about 3 hours and (b) on a textured sample that passed the test. The history of the applied voltage and integrated energy dissipation are also shown. The records confirm visual observations of the way that current is distributed at each of the two types of samples. For the non-textured sample of Figure 7(a), the flow of leakage current is mostly concentrated in this case around electrode 4 and the discharge activity was mostly in the form of an anchored arc causing severe erosion in that area. This behavior is attributed to the restriction of discharge activity within the narrow wet contaminant channel. Periods of no activity are shown too where severe erosion prevented the formation of a complete conductive layer. Figure 7(b) for the textured sample, in contrast, shows higher peak current, but a wider distribution over the composite electrode. The erosion rate is consequently reduced.

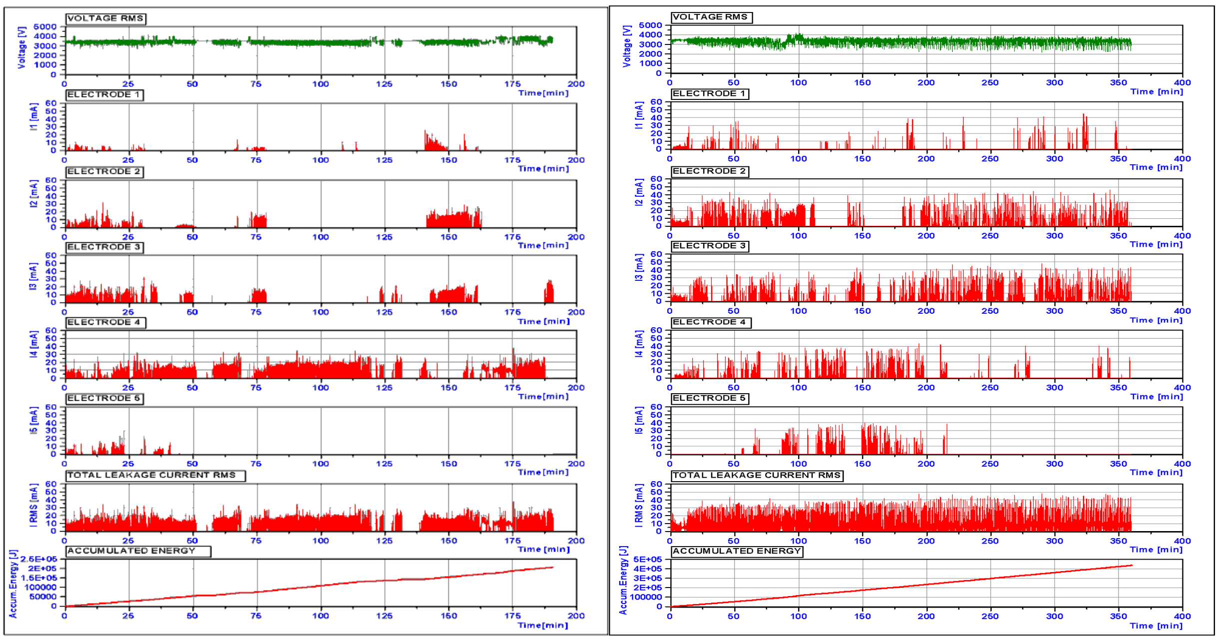

(a) (b)

Figure 7: Isolated-electrode records (a) non-textured sample that failed the test after 3hours (time scale 200min) and (b) 4mm Texture γ sample passing test (time scale 400min).

7 CONCLUSION

- All textured samples successfully passed the inclined-plane tests, which were failed by non-textured samples
- The tracking and erosion rates were reduced significantly for the textured samples.
- The performance of the 4 mm and 6mm square-pattern Texture γ were the most satisfactory.
- Prototype insulators incorporating such textures will be developed.
- For these textures, stable dry bands were formed in the pollution layer which account for the superior test outcome.
- The characterisation of the dry band discharges has enabled breakdown models to be tested [7].

8 ACKNOWLEDGMENTS

The authors would like to thank EPSRC for the financial support (EP/F02844X) of this project.

9 REFERENCES

[1] D.A. Swift, “Insulators for outdoor applications”, Chap.6 in *Advances in High Voltage Engineering* (ed. A.Haddad and D. Warne, IEE Power and Energy Series 40, London, 2004).

[2] IEC 60587: 1984:, “Methods for evaluating resistance to tracking and erosion of electrical insulating materials used under sevre ambient conditions”, IEC standard.

[3] R. T. Waters and A. Haddad, “Insulating Structures”, UK Patent GB2406225B, Dec 2006.

[4] A. Haddad, R.T Waters, H.Griffiths, K.Chrzan, N.Harid, P.Sarkar and P.Charalampidis, “A New Approach to Anti-fog Design for Polymeric Insulators”, IEEE Trans. Dielectr. Electr. Insul. vol. 17, No. 2, pp. 343–350, 2010.

[5] Application Design Patterns: Producer/Consumer, http://zone.ni.com/devzone/cda/tut/p/id/3023., last accessed: May 01, 2011.

[6] Writing TDM and TDMS Files in LabVIEW, http://zone.ni.com/devzone/cda/tut/p/id/9334., last accessed: May 01, 2011.

[7] P. Charalampidis, M. Albano, A. Haddad, R.T Waters, H.Griffiths and N.Harid, “Dry band discharges on silicone rubber insulation”, Proc. 17th Int. Symp. HV Eng. (Hannover, 2011).